

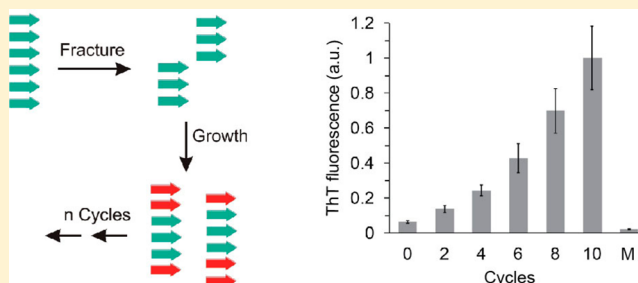
# Amplification of Tau Fibrils from Minute Quantities of Seeds

Virginia Meyer,<sup>†</sup> Paul D. Dinkel,<sup>†</sup> Emily Rickman Hager, and Martin Margittai\*

Department of Chemistry and Biochemistry, University of Denver, Denver, Colorado 80208, United States

## S Supporting Information

**ABSTRACT:** The propagation of Tau pathology in Alzheimer's disease (AD) is thought to proceed through templated conversion of Tau protein into fibrils and cell-to-cell transfer of elongation-competent seeds. To investigate the efficiency of Tau conversion, we adapted the protein misfolding cyclic amplification assay used for the conversion of prions. Utilizing heparin as a cofactor and employing repetitive cycles of shearing and growth, synthetic Tau fibrils and Tau fibrils in AD brain extract are progressively amplified. Concurrently, self-nucleation is suppressed. The results highlight breakage-induced replication of Tau fibrils as a potential facilitator of disease spread.



Tau fibrils, deposited in the interior of nerve cells, are a defining hallmark of Alzheimer's disease (AD) and other fatal neurodegenerative disorders.<sup>1,2</sup> Fibrillar Tau species can transfer between cells and then recruit endogenous Tau proteins onto their ends.<sup>3</sup> Multiple lines of evidence indicate that this mechanism could be responsible for the intracerebral spreading of Tau pathology.<sup>4–8</sup> The template-assisted conversion of Tau monomers into fibrils is reminiscent of the conversion of prions in transmissible spongiform encephalopathies.<sup>9</sup> Little, though, is known about the efficiency of this process.

A unique feature of Tau is that it occurs in six different isoforms.<sup>2</sup> These range between 352 and 441 amino acids in size and can be classified into two principle groups based on the number of microtubule binding repeats. Three-repeat (3R) Tau possesses three semiconserved repeats. Four-repeat (4R) Tau possesses four repeats. The repeat region comprises ~90–120 amino acids and constitutes the core of the Tau fibrils,<sup>10,11</sup> whereas the remaining residues form an unstructured fuzzy coat.<sup>12,13</sup> Fibrils composed of a single Tau isoform can form distinct conformers.<sup>14–16</sup> In a templated reaction, a single conformer may propagate indefinitely, providing a possible explanation for the phenotypic diversity of human tauopathies.<sup>17</sup> The template-assisted reaction, as originally described for brain-derived fibrils,<sup>18</sup> offers a powerful tool to investigate the structure of Tau fibrils. However, the need of large quantities of brain tissue and elaborate protocols to isolate the fibrils have limited its use. For prions, it was shown that repetitive cycles of shearing and growth could amplify the misfolded form, PrP<sup>Sc</sup>.<sup>19</sup> This procedure, which is further potentiated by the inclusion of anionic cofactors,<sup>20</sup> is generally referred to as protein misfolding cyclic amplification (PMCA). It is unknown whether a similar protocol could be adapted for the amplification of Tau fibrils. Different from the prion protein, which has a distinct fold,<sup>21</sup> Tau protein is intrinsically

disordered.<sup>22,23</sup> Furthermore, Tau fibrils are significantly less stable in GdnHCl than PrP<sup>Sc</sup><sup>24,25</sup> and require cofactors for assembly.<sup>26</sup> Despite these differences, we demonstrate that minute quantities of synthetic Tau fibrils can be amplified *in vitro* and in crude brain extracts of AD tissue.

## MATERIALS AND METHODS

**Protein Expression and Purification.** Four constructs of Tau were used in this study: K18, K19, htau40, and htau23.<sup>27</sup> The truncated versions of Tau were chosen to represent only the core of the fibril (K18 for 4R Tau and K19 for 3R Tau).<sup>27</sup> All Tau proteins were expressed and purified according to previously described protocols.<sup>27,28</sup> Specifically, cultures of pET28-containing BL21 (DE3) *Escherichia coli* bacteria in Miller LB broth with 20  $\mu$ g/mL kanamycin were incubated at 37 °C under agitation for 16–17 h. This was then diluted 1:100 into fresh medium, and incubation was continued until the optical density of the solution reached ~0.8 at 600 nm. One millimolar isopropyl- $\beta$ -D-thiogalactopyranoside (IPTG, Gold Biotechnology) was added to induce protein expression, which continued at 37 °C for 3.5–4 h. The cells were pelleted at 3000g and resuspended in buffer (20 mM piperazine-*N,N'*-bis(2-ethanesulfonic acid) (PIPES, J.T. Baker), pH 6.5, 500 mM NaCl, 1 mM ethylenediaminetetraacetic acid (EDTA, J.T. Baker), and 50 mM  $\beta$ -mercaptoethanol (MP Biomedicals)). Resuspended bacteria were stored at –80 °C until purification.

Cells were heated at 80 °C for 20 min and then sonicated to fracture the cell walls. Cellular debris was removed by centrifugation at 15 000g for 30 min, after which the supernatant was added to 55% w/v ammonium sulfate. Tau precipitated during room temperature incubation for 1 h and was isolated by centrifugation at 15 000g for 10 min. Pellets

Received: July 17, 2014

Published: August 25, 2014

were resuspended in water with 2 mM dithiothreitol (DTT, Gold Biotechnology). Samples were passed through a 0.45  $\mu\text{m}$  Acrodisc GxP/GHP filter (Pall Life Sciences) before application onto a Mono S cation exchange column (GE Healthcare). Protein was eluted via a linear salt gradient (50–1000 mM NaCl, 20 mM PIPES, pH 6.5, 2 mM DTT). Fractions containing the highest concentration of protein were determined by SDS-PAGE and combined. The pooled fractions were applied onto a Superdex 200 gel filtration column (GE Healthcare) and eluted with 20 mM Tris, 100 mM NaCl, 1 mM EDTA, and 2 mM DTT buffer at pH 7.4. Pure Tau was precipitated at 4 °C overnight by addition of an excess of acetone (K18 and K19) or methanol (htau23 and htau40). Protein was pelleted at 15 000g and stored in 2 mM DTT acetone at –80 °C.

Tau was monomerized by dissolving the protein pellets in 200  $\mu\text{L}$  of 8 M guanidine hydrochloride (Thermo Scientific). This was passed over a PD-10 column (GE Healthcare) to remove denaturant. Protein was eluted with 10 mM 4-(2-hydroxyethyl)-1-piperazineethanesulfonic acid (HEPES, J.T. Baker), 100 mM NaCl, and 1 mM  $\text{NaN}_3$  buffer at pH 7.4, and concentrations were determined using a bicinchoninic (BCA) assay (Pierce).

**Brain Homogenate Preparation.** The brain tissues used in this project (AD and tangle-free control) were provided by the University of California Alzheimer's Disease Research Center (UCI-ADRC) and the Institute for Memory Impairments and Neurological Disorders. Brain tissue was diluted 5-fold with a solution of 5 mM EDTA and 10 mM HEPES buffer at pH 7.4. The mixture was homogenized in a Potter–Elvehjem tissue grinder at 250 rpm using SteadyStir Digital (Fisher Scientific) for 5 min, followed by centrifugation for 20 min at 16 500g. Supernatant was removed, and the pellet was resuspended in 2-fold buffer volume. The mixture was homogenized again with the same settings. All steps were performed at 4 °C. Protein concentration of total brain homogenate was determined using a BCA assay. Aliquots were flash frozen and stored at –80 °C until used.

**Amplification of Synthetic Tau Fibrils.** Sonication cycles (the number of cycles depended on experiment and is specified in the Results section) were achieved using a bath sonicator in which a water-filled microplate horn was coupled to an ultrasonic processor (QSonica). A single cycle consisted of 5 s sonication pulses at 5% amplitude. The water temperature was held constant at 37 °C using a recirculating chiller for the incubation cycles, which were 30 min. The reactions were contained within Nunclon 96-well plates (Thermo Scientific) and were covered with BioDot Microplate sealing tape (Dot Scientific). Each well in the microplate corresponded to an individual experiment. Thioflavin T (ThT, Sigma) was used as the fluorescent indicator of fibril growth. The following were added to each well: 10  $\mu\text{M}$  Tau monomer (htau40 or htau23), 40  $\mu\text{M}$  heparin (Celsus, average MW = 5000), 5  $\mu\text{M}$  ThT, appropriate concentration of seeds, and additional buffer (100 mM NaCl, 10 mM HEPES, pH 7.4) to make the total sample volume 200  $\mu\text{L}$ .

Control wells were run alongside each experiment. A monomer control contained all components except seeds to show that aggregation of the reaction wells occurred through amplification, not through spontaneous nucleation. A ThT-only control was also run to determine the background fluorescent signal of the dye. This background was subtracted from the experimental signal. Seeds were formed from K18 and K19 by

stirring 25  $\mu\text{M}$  monomer with 12.5  $\mu\text{M}$  heparin for 3 days at room temperature. Htau40 and htau23 were formed analogously but were stirred for 8 days because fibril growth is slower for full-length Tau. All microplate experiments involved diluting the initial seeds, which was done using buffer and 40  $\mu\text{M}$  heparin to ensure fibrils remained intact. Seeds were added to reactions prior to incubation or sonication cycling and were present according to the molar percentage of seed per monomeric Tau, 10  $\mu\text{M}$  for all experiments.

Buoyant bulbs were attached to either side of the microplates to prevent sinking into the sonicator bath. Following amplification, the plate was centrifuged at 1650g for 2 min to remove condensation from the sealing tape. Fluorescence was immediately measured using a Tecan Infinite M1000 microplate reader. ThT was excited at 440 nm, and spectra were collected by scanning emission from 450–530 nm in 5 nm steps. The Z position of the plate within the reader was kept constant. Quantification of Tau aggregation was determined by ThT emission at 480 nm.

In addition to ThT as a fluorescent readout, fibrils were sedimented and analyzed on an SDS-PAGE gel to monitor amplification over successive cycles. Experiments were performed by preparing four microplate wells with the same components. Following ThT measurement, these wells were pooled and centrifuged at 100 000g for 30 min at 10 °C. Pellets were washed with 1 mL of buffer, dissolved in 75  $\mu\text{L}$  of 1 $\times$  SDS-PAGE sample buffer, and run on a corresponding gel.

Using the techniques outlined here, htau40 proceeded ~60 cycles before spontaneous monomer growth, as indicated by control experiments in which fibril seeds were excluded. Htau23, which grew less efficiently than htau40, could undergo ~80 cycles before spontaneous monomer growth.

#### **Amplification of Tau Fibrils from Brain Homogenate.**

Experimental parameters were altered for use on brain tissue to account for interference from extracellular components. Reactions were carried out with 5  $\mu\text{M}$  htau40 and 20  $\mu\text{M}$  heparin in buffer (100 mM NaCl, 10 mM HEPES, pH 7.4). Brain tissue homogenate was prepared for amplification by creating a 10% dilution using reaction buffer followed by the addition of 0.1% Triton X-100. The homogenate was then sonified in the bath sonicator at 5% amplitude for 60 s. A total weight of 20  $\mu\text{g}$  of brain tissue (protein mass) was added to each 200  $\mu\text{L}$  final reaction volume. Using the same power settings as those with recombinant material, 20 cycles of sonication and incubation were performed.

#### **Negative Stain Transmission Electron Microscopy.**

200-mesh carbon-coated copper grids were placed for 1 min onto 10  $\mu\text{L}$  drops of sample (5  $\mu\text{M}$  of fibrils based on monomer concentration) and then for 30 s onto 10  $\mu\text{L}$  drops of 2% uranyl acetate. The grids were air-dried on filter paper. Images were taken with a Philips/FEI Tecnai-12 electron transmission microscope at 80 keV, equipped with a Gatan CCD camera.

**Variability in Amplification.** Identical reactions performed in multiple wells in the microplate displayed varying amounts of ThT fluorescence, as reflected by error bars. Emission spectra indicate that the variability in amplification can arise, sometimes deviating due to a single reaction. It is possible that this variability originates due to an uneven force distribution in the bath, a finding that was suggested previously.<sup>20</sup> Slight variability was also seen in the power output of different bath sonicators.

## RESULTS

**Amplification of Tau Fibrils through Cycles of Seeding and Growth.** In a first set of experiments, we tested the effect of seed concentration on fibril growth. Specifically, httau40 (the largest isoform of Tau) was seeded with sonicated fibrils composed of K18. Fibril growth was monitored by ThT fluorescence.<sup>16</sup> As expected, ThT displayed decreasing fluorescence with decreasing seed concentration, indicating diminished formation of fibrils (Figure 1). Importantly,

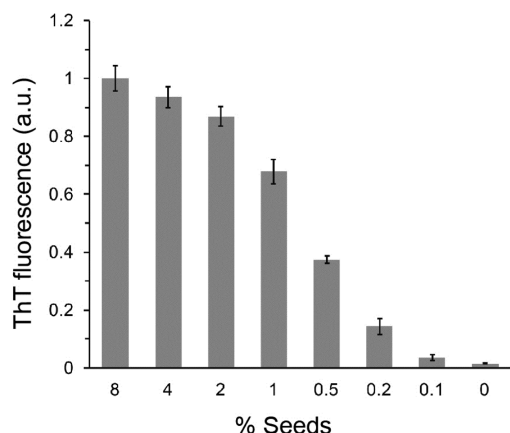


**Figure 1.** Seeding of Tau monomer with varying seed concentrations. Various concentrations of K18 fibril seeds were added to recruit monomeric Tau. Monomeric httau40 (10  $\mu$ M) was incubated with seeds and 5  $\mu$ M ThT for 6 h. Fluorescence emission was measured at 480 nm, with excitation at 440 nm. Heparin was included in all reactions at a concentration of 40  $\mu$ M. All values represent mean  $\pm$  SEM ( $n = 4$ ).

incubation of monomers without the addition of seeds produced no fibrils. At the lowest seed concentration of 0.1% (monomer equivalents), fibril elongation is extremely inefficient (Figure 1). We therefore examined if inclusion of regular

sonication steps during incubation could amplify fibrils at this seed concentration. The rationale for employing cycles of sonication is to provide a larger number of fibril ends per unit mass. The increase in Tau fibril ends through fragmentation has been recognized as the main effect of sonication.<sup>29</sup> Repetitive cycles of shearing and growth could thus increase the number of monomers converted (Figure 2A). To suppress self-nucleation of Tau monomers, which is accelerated by the formation of intermolecular disulfide bonds,<sup>18,30,31</sup> in these and all other experiments, Tau constructs were used with natural cysteines replaced by serines (one cysteine in 3R Tau and two cysteines in 4R Tau). Amplification was monitored by ThT fluorescence over 10 cycles (a single cycle consists of 5 s of sonication followed by 30 min of incubation at 37  $^{\circ}$ C). Amplification was monitored every two cycles, during which ThT fluorescence steadily increased with additional cycles (Figure 2B). Using sedimentation, the amplified httau40 fibrils were also visualized on an SDS-PAGE gel (Figure 2C). The gel corroborates the ThT results showing consistent amplification with increasing cycles. The total 5 h incubation time for 10 cycles demonstrates considerable fibril amplification onto 0.1% seeds compared to 6 h of incubation following a single sonication step (Figure 1). Seeds of 3R Tau (K19) were also amplified using httau23 (Figure S1 of the Supporting Information), although this process was consistently less efficient, requiring additional cycles of sonication and growth.

**Sensitivity of Tau Amplification.** The amplification protocol shows significant enhancement in fibril concentration over incubation alone for 0.1% initial seeds. The initial seeds were further diluted to characterize the sensitivity of this technique. Htttau40 monomer was added to K18 seeds ranging from 0.1 to 0.00001% of the monomer concentration, and 40 cycles of shearing were applied. Amplification decreased proportionately with seed concentration (Figure 3A), showing no fibril growth from the monomer alone. Similar amplification was seen using these concentrations of httau40 seeds added to httau40 monomer (Figure 3B). To ensure fibrillar structure was

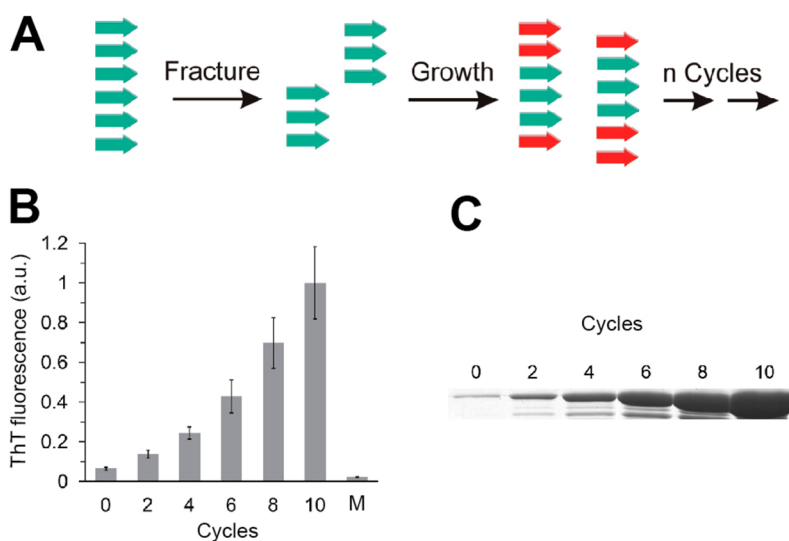


**Figure 2.** Amplification of Tau fibrils. (A) Flowchart. Green arrows represent  $\beta$ -strands in the original fibril. Red arrows represent  $\beta$ -strands of newly incorporated monomers. A single cycle involves consecutive steps of fibril fracture and growth. (B) 0.1% K18 seeds were added to httau40 and amplified over 10 cycles of sonication and growth. The degree of amplification was monitored by ThT fluorescence and (C) visualized by Coomassie-staining following fibril sedimentation. M = monomer control subjected to 10 cycles of shearing and growth. Values represent mean  $\pm$  SEM ( $n = 8$ ).

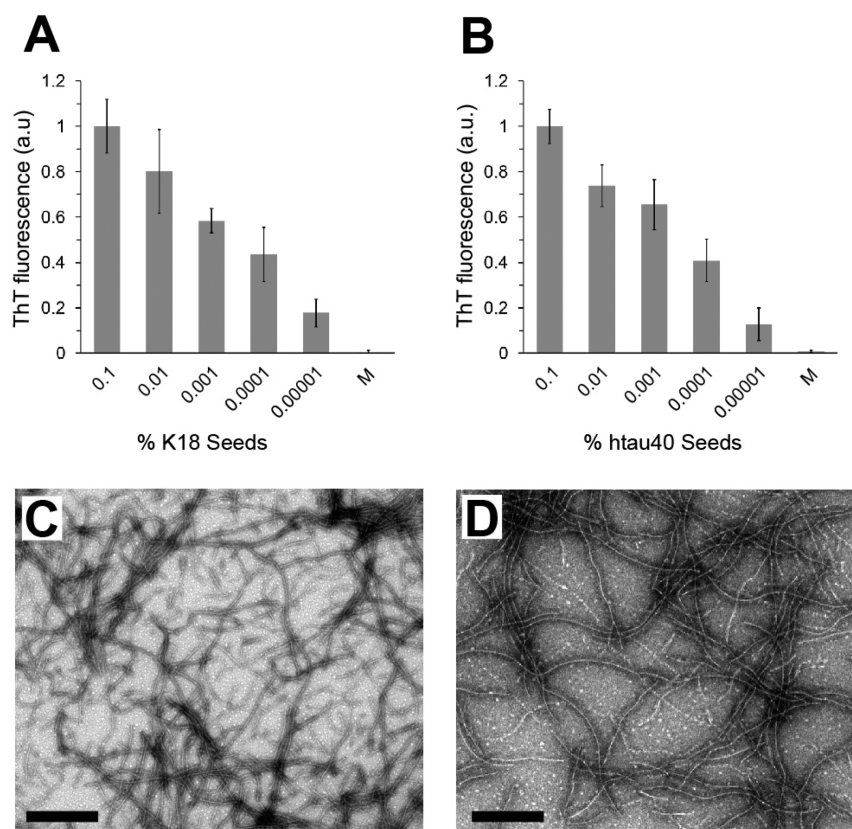


**Figure 3.** Sensitivity of amplification. Initial seeds were diluted and amplified with htau40 using 40 cycles of shearing and growth. The degree of amplification decreases linearly with decreasing seed concentration for both K18 seeds (A) and htau40 seeds (B). EM images show the extended htau40 fibrils formed using 0.1% K18 seeds (C) and 0.1% htau40 seeds (D). Scale bars = 500 nm. M = monomer control subjected to 40 cycles of shearing and growth. Values in panels A and B represent mean  $\pm$  SEM ( $n = 8$ ).

the source of increased ThT fluorescence, fibrils grown from 0.1% seeds following 40 shearing cycles were visualized by EM (Figure 3C,D). PMCA has been shown to be a remarkably sensitive technique for the amplification of PrP<sup>Sc</sup>,<sup>32</sup> and we have demonstrated here that a high sensitivity can also be achieved for Tau fibrils. The lowest seed concentration amplified in Figure 3A,B corresponds to 1 pM protein. It is expected that additional improvements in the assay could enhance the sensitivity further.

K19 and htau23 seeds could also be diluted and amplified with htau23 using the same experimental parameters as were used for htau40. The extent of amplification at low seed concentrations, however, was decreased for htau23 compared to that for htau40 (Figure S2 of the Supporting Information). This could reflect a lower stability of the htau23 fibrils and underscores the reduced efficiency of htau23 amplification.

**Amplification of Tau Fibrils from AD-Derived Brain Tissue.** One of the greatest strengths of PMCA is the ability to amplify protein aggregates from biological samples. To demonstrate this feature using Tau protein, AD brain and tangle-free control brain were homogenized, diluted, and then added to recombinant htau40. Next, the samples were subjected to 20 cycles of amplification, with each cycle consisting of 5 s of sonication and 30 min of incubation at 37 °C. ThT could not be used for detection because it interacts with RNA, DNA, and other cellular components in the brain homogenate. We therefore visualized Tau amplification by sedimentation using SDS-PAGE. Only the sample that contained AD extract was able to template growth (Figure

4A, lane 5). Importantly, spontaneous nucleation could be excluded, as neither htau40 alone nor htau40 in the presence of control brain caused aggregation (Figure 4A, lanes 1 and 4). Furthermore, both AD brain and tangle-free control brain showed similar banding patterns (Figure 4A, lanes 2 and 3), highlighting the overall analogous protein compositions. The fibrillar nature of the amplified protein aggregates was verified by EM (Figure 4B). Importantly, AD brain extract alone, i.e., in the absence of recombinant Tau, did not show any fibrils (Figure 4C). Combined, the findings indicate that Tau fibrils can be selectively amplified from Tau seeds inherent in the crude AD brain extract.

## DISCUSSION

In Alzheimer's disease and related neurodegenerative disorders, Tau protein is deposited in the form of large neurofibrillary tangles. These are bundles of long, unbranched filaments that are poor candidates for disease propagation. Our findings demonstrate that repetitive cycles of shearing and growth dramatically enhance the conversion of monomeric Tau into fibrils. Fibril fragmentation may be the central mechanism in this procedure. However, other secondary pathways<sup>33,34</sup> such as branching<sup>35</sup> or heterogeneous nucleation from the fibril surface<sup>36,37</sup> may also contribute to enhanced aggregation. If latter processes were operative, then they would be expected to add to the conformational heterogeneity of Tau fibril populations.<sup>38</sup>

The biological mechanisms that produce smaller Tau aggregates in the cell are not understood. Such mechanisms,

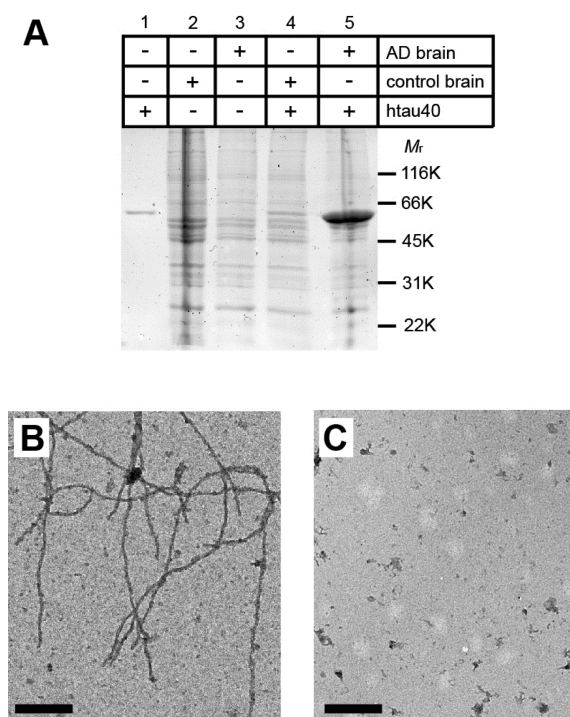


**Figure 4.** Seeding of Tau monomers with brain extract. (A) 5  $\mu$ M htau40 and 20  $\mu$ g of brain extract were combined as indicated (total volume = 200  $\mu$ L). All combinations were carried through 20 cycles of shearing and growth. The proteins were then sedimented and analyzed by SDS-PAGE and Coomassie staining. Only monomers that were seeded with AD extract produced htau40 aggregates, as indicated by the dark band in lane 5. (B) EM image of htau40 fibrils seeded with AD brain extract. (C) EM image of AD brain extract in the absence of recombinant Tau. Scale bars = 500 nm.

however, must exist. Only small aggregates possess the capacity to be taken up by cells.<sup>39</sup> Similarly, only fibrils that are released from the cell will be able to act in trans-cellular propagation.<sup>3</sup> Once taken up by the target cell, fibrils have to fracture to provide new surface area for monomer recruitment to the fibril ends. Efficient replication could hence depend on the facility of these fibrils to break. Interestingly, a correlation between aggregate brittleness and strain propagation has been observed for yeast prions, where more fragile conformers (or strains) have a selective advantage.<sup>40</sup> In these organisms, the molecular chaperone, HSP104, in conjunction with additional factors, is thought to provide the mechanical force that fractures the fibrils and allows segregation of smaller aggregates into daughter cells.<sup>41</sup> A homologue of HSP104, however, does not exist in mammalian cells. Whether molecular chaperones mediate the breakage of Tau fibrils is unknown. It is possible that another clearance-related mechanism could cause fracture or that multiple mechanisms operate in parallel. Regardless of the molecular details of these processes, fibril fracture appears to be a critical part of replication. The herein developed *in vitro* assay offers a powerful new tool for amplifying Tau fibrils from crude brain extract and investigating their conformations. Further enhancements in sensitivity could transform this assay into a potentially valuable diagnostic tool.

■ ASSOCIATED CONTENT

📄 Supporting Information

Amplification of 3R Tau fibrils and sensitivity of amplification for htau23 grown onto K19 and htau23 seeds. This material is available free of charge via the Internet at <http://pubs.acs.org>.

■ AUTHOR INFORMATION

Corresponding Author

\*Tel.: (303) 871-4135; Fax: (303) 871-2254; E-mail: martin.margittai@du.edu.

Author Contributions

†V.M. and P.D.D. contributed equally to this work.

Funding

This project was supported by NIH/NINDS grant no. R01NS076619 (to M.M.). The UCI-ADRC, which provided brain samples for this project, is funded by NIH/NIA grant no. P50 AG16573.

Notes

The authors declare no competing financial interest.

■ REFERENCES

- (1) Lee, V. M., Goedert, M., and Trojanowski, J. Q. (2001) Neurodegenerative tauopathies. *Annu. Rev. Neurosci.* 24, 1121–1159.
- (2) Spillantini, M. G., and Goedert, M. (2013) Tau pathology and neurodegeneration. *Lancet Neurol.* 12, 609–622.
- (3) Kfoury, N., Holmes, B. B., Jiang, H., Holtzman, D. M., and Diamond, M. I. (2012) Trans-cellular Propagation of Tau Aggregation by Fibrillar Species. *J. Biol. Chem.* 287, 19440–19451.
- (4) de Calignon, A., Polydoro, M., Suarez-Calvet, M., William, C., Adamowicz, D. H., Kopeikina, K. J., Pittstick, R., Sahara, N., Ashe, K. H., Carlson, G. A., Spire-Jones, T. L., and Hyman, B. T. (2012) Propagation of tau pathology in a model of early Alzheimer's disease. *Neuron* 73, 685–697.
- (5) Liu, L., Drouet, V., Wu, J. W., Witter, M. P., Small, S. A., Clelland, C., and Duff, K. (2012) Trans-synaptic spread of tau pathology in vivo. *PLoS One* 7, e31302.
- (6) Clavaguera, F., Akatsu, H., Fraser, G., Crowther, R. A., Frank, S., Hench, J., Probst, A., Winkler, D. T., Reichwald, J., Staufenbiel, M., Ghetti, B., Goedert, M., and Tolnay, M. (2013) Brain homogenates from human tauopathies induce tau inclusions in mouse brain. *Proc. Natl. Acad. Sci. U.S.A.* 110, 9535–9540.
- (7) Iba, M., Guo, J. L., McBride, J. D., Zhang, B., Trojanowski, J. Q., and Lee, V. M. (2013) Synthetic tau fibrils mediate transmission of neurofibrillary tangles in a transgenic mouse model of Alzheimer's-like tauopathy. *J. Neurosci.* 33, 1024–1037.
- (8) Clavaguera, F., Bolmont, T., Crowther, R. A., Abramowski, D., Frank, S., Probst, A., Fraser, G., Stalder, A. K., Beibel, M., Staufenbiel, M., Jucker, M., Goedert, M., and Tolnay, M. (2009) Transmission and spreading of tauopathy in transgenic mouse brain. *Nat. Cell Biol.* 11, 909–913.
- (9) Prusiner, S. B. (1998) Prions. *Proc. Natl. Acad. Sci. U.S.A.* 95, 13363–13383.
- (10) Wischik, C. M., Novak, M., Thogersen, H. C., Edwards, P. C., Runswick, M. J., Jakes, R., Walker, J. E., Milstein, C., Roth, M., and Klug, A. (1988) Isolation of a fragment of tau derived from the core of the paired helical filament of Alzheimer disease. *Proc. Natl. Acad. Sci. U.S.A.* 85, 4506–4510.
- (11) Novak, M., Kabat, J., and Wischik, C. M. (1993) Molecular characterization of the minimal protease resistant tau unit of the Alzheimer's disease paired helical filament. *EMBO J.* 12, 365–370.
- (12) Wischik, C. M., Novak, M., Edwards, P. C., Klug, A., Tichelaar, W., and Crowther, R. A. (1988) Structural characterization of the core of the paired helical filament of Alzheimer disease. *Proc. Natl. Acad. Sci. U.S.A.* 85, 4884–4888.
- (13) Wegmann, S., Medalsy, I. D., Mandelkow, E., and Muller, D. J. (2013) The fuzzy coat of pathological human Tau fibrils is a two-

layered polyelectrolyte brush. *Proc. Natl. Acad. Sci. U.S.A.* 110, E313–E321.

(14) Frost, B., Ollesch, J., Wille, H., and Diamond, M. I. (2009) Conformational diversity of wild-type Tau fibrils specified by templated conformation change. *J. Biol. Chem.* 284, 3546–3551.

(15) Siddiqua, A., Luo, Y., Meyer, V., Swanson, M. A., Yu, X., Wei, G., Zheng, J., Eaton, G. R., Ma, B., Nussinov, R., Eaton, S. S., and Margittai, M. (2012) Conformational basis for asymmetric seeding barrier in filaments of three- and four-repeat tau. *J. Am. Chem. Soc.* 134, 10271–10278.

(16) Dinkel, P. D., Siddiqua, A., Huynh, H., Shah, M., and Margittai, M. (2011) Variations in filament conformation dictate seeding barrier between three- and four-repeat Tau. *Biochemistry* 50, 4330–4336.

(17) Sanders, D. W., Kaufman, S. K., DeVos, S. L., Sharma, A. M., Mirbaha, H., Li, A., Barker, S. J., Foley, A. C., Thorpe, J. R., Serpell, L. C., Miller, T. M., Grinberg, L. T., Seeley, W. W., and Diamond, M. I. (2014) Distinct tau prion strains propagate in cells and mice and define different tauopathies. *Neuron* 82, 1271–1288.

(18) Friedhoff, P., von Bergen, M., Mandelkow, E. M., Davies, P., and Mandelkow, E. (1998) A nucleated assembly mechanism of Alzheimer paired helical filaments. *Proc. Natl. Acad. Sci. U.S.A.* 95, 15712–15717.

(19) Saborio, G. P., Permanne, B., and Soto, C. (2001) Sensitive detection of pathological prion protein by cyclic amplification of protein misfolding. *Nature* 411, 810–813.

(20) Deleault, N. R., Harris, B. T., Rees, J. R., and Supattapone, S. (2007) Formation of native prions from minimal components in vitro. *Proc. Natl. Acad. Sci. U.S.A.* 104, 9741–9746.

(21) Riek, R., Hornemann, S., Wider, G., Billeter, M., Glockshuber, R., and Wuthrich, K. (1996) NMR structure of the mouse prion protein domain PrP(121–231). *Nature* 382, 180–182.

(22) Cleveland, D. W., Hwo, S. Y., and Kirschner, M. W. (1977) Physical and chemical properties of purified tau factor and the role of tau in microtubule assembly. *J. Mol. Biol.* 116, 227–247.

(23) Mukrasch, M. D., Bibow, S., Korukottu, J., Jeganathan, S., Biernat, J., Griesinger, C., Mandelkow, E., and Zweckstetter, M. (2009) Structural polymorphism of 441-residue tau at single residue resolution. *PLoS Biol.* 7, e34.

(24) Li, L., von Bergen, M., Mandelkow, E. M., and Mandelkow, E. (2002) Structure, stability, and aggregation of paired helical filaments from tau protein and FTDP-17 mutants probed by tryptophan scanning mutagenesis. *J. Biol. Chem.* 277, 41390–41400.

(25) Legname, G., Nguyen, H. O., Peretz, D., Cohen, F. E., DeArmond, S. J., and Prusiner, S. B. (2006) Continuum of prion protein structures enciphers a multitude of prion isolate-specified phenotypes. *Proc. Natl. Acad. Sci. U.S.A.* 103, 19105–19110.

(26) Kuret, J., Congdon, E. E., Li, G., Yin, H., Yu, X., and Zhong, Q. (2005) Evaluating triggers and enhancers of tau fibrillization. *Microsc. Res. Technol.* 67, 141–155.

(27) Siddiqua, A., and Margittai, M. (2010) Three- and four-repeat Tau coassemble into heterogeneous filaments: an implication for Alzheimer disease. *J. Biol. Chem.* 285, 37920–37926.

(28) Margittai, M., and Langen, R. (2004) Template-assisted filament growth by parallel stacking of tau. *Proc. Natl. Acad. Sci. U.S.A.* 101, 10278–10283.

(29) Ramachandran, G., and Udgaonkar, J. B. (2012) Evidence for the existence of a secondary pathway for fibril growth during the aggregation of tau. *J. Mol. Biol.* 421, 296–314.

(30) Schweers, O., Mandelkow, E. M., Biernat, J., and Mandelkow, E. (1995) Oxidation of cysteine-322 in the repeat domain of microtubule-associated protein tau controls the in vitro assembly of paired helical filaments. *Proc. Natl. Acad. Sci. U.S.A.* 92, 8463–8467.

(31) Furukawa, Y., Kaneko, K., and Nukina, N. (2011) Tau protein assembles into isoform- and disulfide-dependent polymorphic fibrils with distinct structural properties. *J. Biol. Chem.* 286, 27236–27246.

(32) Saa, P., Castilla, J., and Soto, C. (2006) Ultra-efficient replication of infectious prions by automated protein misfolding cyclic amplification. *J. Biol. Chem.* 281, 35245–35252.

(33) Bishop, M. F., and Ferrone, F. A. (1984) Kinetics of nucleation-controlled polymerization. A perturbation treatment for use with a secondary pathway. *Biophys. J.* 46, 631–644.

(34) Ferrone, F. (1999) Analysis of protein aggregation kinetics. *Methods Enzymol.* 309, 256–274.

(35) Andersen, C. B., Yagi, H., Manno, M., Martorana, V., Ban, T., Christiansen, G., Otzen, D. E., Goto, Y., and Rischel, C. (2009) Branching in amyloid fibril growth. *Biophys. J.* 96, 1529–1536.

(36) Cohen, S. I., Linse, S., Luheshi, L. M., Hellstrand, E., White, D. A., Rajah, L., Otzen, D. E., Vendruscolo, M., Dobson, C. M., and Knowles, T. P. (2013) Proliferation of amyloid-beta2 aggregates occurs through a secondary nucleation mechanism. *Proc. Natl. Acad. Sci. U.S.A.* 110, 9758–9763.

(37) Buell, A. K., Galvagnion, C., Gaspar, R., Sparr, E., Vendruscolo, M., Knowles, T. P., Linse, S., and Dobson, C. M. (2014) Solution conditions determine the relative importance of nucleation and growth processes in alpha-synuclein aggregation. *Proc. Natl. Acad. Sci. U.S.A.* 111, 7671–7676.

(38) Meyer, V., Dinkel, P. D., Luo, Y., Yu, X., Wei, G., Zheng, J., Eaton, G. R., Ma, B., Nussinov, R., Eaton, S. S., and Margittai, M. (2014) Single mutations in tau modulate the populations of fibril conformers through seed selection. *Angew. Chem., Int. Ed.* 53, 1590–1593.

(39) Wu, J. W., Herman, M., Liu, L., Simoes, S., Acker, C. M., Figueroa, H., Steinberg, J. I., Margittai, M., Kaye, R., Zurzolo, C., Di Paolo, G., and Duff, K. E. (2013) Small misfolded Tau species are internalized via bulk endocytosis and anterogradely and retrogradely transported in neurons. *J. Biol. Chem.* 288, 1856–1870.

(40) Tanaka, M., Collins, S. R., Toyama, B. H., and Weissman, J. S. (2006) The physical basis of how prion conformations determine strain phenotypes. *Nature* 442, 585–589.

(41) Doyle, S. M., Genest, O., and Wickner, S. (2013) Protein rescue from aggregates by powerful molecular chaperone machines. *Nat. Rev. Mol. Cell Biol.* 14, 617–629.